Pediatr Radiol (2015) 45:1056–1065
DOI 10.1007/s00247-014-3239-y

PICTORIAL ESSAY

CT and MRI of congenital nasal lesions in syndromic conditions

Daniel T. Ginat · Caroline D. Robson

Received: 1 April 2014 / Revised: 1 October 2014 / Accepted: 12 November 2014 / Published online: 9 January 2015

Abstract Congenital malformations of the nose can be associated with a variety of syndromes, including solitary median maxillary central incisor syndrome, CHARGE syndrome, Bosma syndrome, median cleft face syndrome, PHACES association, Bartsocas-Papas syndrome, Binder syndrome, duplication of the pituitary gland-plus syndrome and syndromic craniosynsotosis (e.g., Apert and Crouzon syndromes) among other craniofacial syndromes. Imaging with CT and MRI plays an important role in characterizing the nasal anomalies as well as the associated brain and cerebrovascular lesions, which can be explained by the intimate developmental relationship between the face and intracranial structures, as well as certain gene mutations. These conditions have characteristic imaging findings, which are reviewed in this article.

Keywords Nose · Congenital · Syndrome · Imaging · Magnetic resonance imaging · Computed tomography · Children

Introduction

Several uncommon syndromes are associated with congenital anomalies of the nasal region that can manifest with various forms of nasal aplasia, choanal atresia, pyriform aperture stenosis, midface hypoplasia and frontonasal masses. Neuroimaging is important not only for characterization of the nasal lesions, but it is also indispensable for the evaluation of associated craniofacial, intracranial and cerebrovascular malformations. CT and MRI have complimentary roles in the work-up of these conditions. High-resolution maxillofacial CT is useful for delineating the underlying abnormal osseous anatomy, while MRI and MR angiography are best suited for evaluating associated intracranial structural abnormalities and cerebrovascular lesions, respectively [1]. The embryology pertaining to the nose and the neuroimaging features of various conditions associated with congenital anomalies of the nose, including solitary median maxillary central incisor syndrome, CHARGE syndrome, Bosma syndrome, median cleft face syndrome, PHACES association, Bartsocas-Papas syndrome and duplication of the pituitary gland-plus syndrome and craniofacial syndromes, such as Antley-Bixler, Apert and Crouzon syndromes, are reviewed in the following sections.

D. T. Ginat (✉)
Department of Radiology, University of Chicago,
5841 S. Maryland Ave., Chicago, IL 60637, USA
e-mail: ginatd01@gmail.com

C. D. Robson
Department of Radiology, Boston Children's Hospital,
Harvard Medical School,
Boston, MA, USA

Embryology of the nose

The prosencephalon (embryonic forebrain) arises from a mesenchymal matrix of local paraxial mesoderm and of neural crest cells derived from the posterior diencephalon and mesencephalon [2]. The frontonasal region derives mesenchyme from two regions of neural crest cells: The midbrain neural crest cells migrate to form the lateral nasal process, while the forebrain neural crest cells form the medial nasal processes [3, 4]. The nose and nasal cavity form between 4 and 10 weeks of gestation, in which the lateral nasal processes join the maxillary process to form the lateral nose and nasolacrimal groove and the medial nasal and maxillary processes join to form the philtrum and columella medially and the bucconasal groove and membrane laterally (Fig. 1) [3, 4]. The medial and lateral nasal processes form the boundaries of the nasal pits, which gradually extend farther posteriorly within the mesenchyme, eventually leaving a thin sheet of tissue known as the nasobuccal membrane [5]. This membrane normally

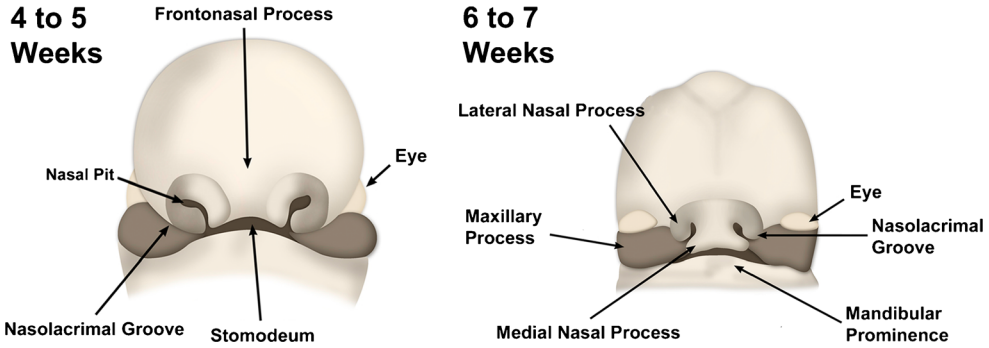

Fig. 1 Schematic of frontonasal region in embryological development. The maxillary prominences and median nasal prominences progressively migrate toward the midline. The nose forms from fusion of the medial and lateral nasal prominences. The upper lip forms from the fusion of the medial nasal prominence and maxillary prominence on each side. The nasolacrimal grooves form as a gap between the lateral nasal prominence and the maxillary prominence

perforates to create a nasal cavity with the primitive choana. As further fusion between the septal elements and palate ensues, the choana moves from its original position more posteriorly to form the permanent choana.

Portions of the presphenoid cartilage give rise to the mesethmoid cartilage, which forms the central portion of the anterior skull base, including the perpendicular plate of the ethmoid bone and the crista galli [6]. During the eighth week of gestation, a transient fontanelle between the inferior frontal bone and nasal bone (fonticulus frontalis) forms and a dural projection extends inferiorly and anteriorly through a midline gap in the anterior skull base anterior to the crista galli (foramen cecum) (Fig. 2). The dural diverticulation extends inferior and posterior to the frontal and nasal bones and superior and anterior to the nasal cartilage (prenasal space). The apex of this dural diverticulation temporarily approximates the subcutaneous region of the mid-nasal bridge at the osteocartilaginous junction [7]. The nasal process of frontal bone, nasal bone and ethmoid bones remains unossified up to the eighth month of life and the soft-tissue attenuation of these structures should not be misinterpreted as a skull base defect [7]. Likewise, the presence of secretions within the nasal cavity juxtaposed against the unossified anterior skull base could potentially be misinterpreted as cephalocele on CT [7]. On the other hand, T2-weighted MRI sequences can readily delineate the inferior frontal lobes, cerebral spinal fluid, ethmoid air cells and crista galli in infants.

Pyriform aperture stenosis in solitary median maxillary central incisor syndrome

Solitary median maxillary central incisor syndrome (SMMCI) is characterized by pyriform aperture stenosis and a solitary median maxillary central incisor, associated with holoprosencephaly. SMMCI syndrome is also associated with hypopituitarism, hypotelorism and other organ system anomalies [8]. The syndrome is considered by some to represent a form of holoprosencephaly that is linked to a mutation of the sonic hedgehog gene (SHH) on chromosome 7q36 and occurs in approximately 1:50,000 live births [8, 9]. The SHH gene directs the interaction between the notochordal plate, the

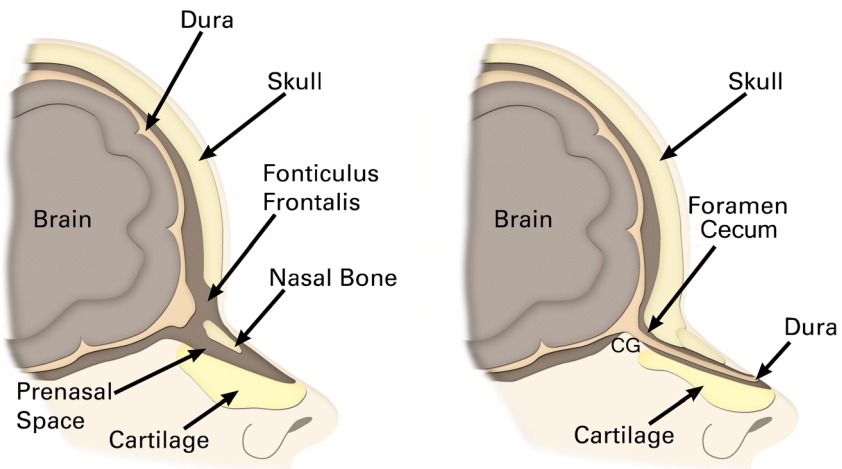

Fig. 2 Schematic of anterior skull base embryology. The fonticulus frontalis represents a gap between the nasal bones and frontal bone, while the foramen cecum is a channel that passes through the ethmoid roof in the midline, anterior to the crista galli (CG)

neuroectoderm, the brain plate and the oral plate. A deficient notochordal plate may inhibit lateral movement of the neuroectoderm. In particular, congenital pyriform aperture stenosis results from narrowing of the nasal processes of the maxilla, which ossify at 4 months of gestation [10]. Similarly, solitary median maxillary central incisor results from the absence of or reduction in lateral growth from the midline during the sixth week of gestation, leading to premature fusion of the epithelial dental lamina, thus preventing the formation of two complete and separate central incisor teeth [9]. Stenosis of the pyriform aperture can be defined as a distance between the lateral rims of the pyriform apertures of less than 11 mm and can be suggested by difficulty in passing a small catheter or nasogastric tube through the anterior nasal apertures [11, 12]. High-resolution CT, particularly axial sections, is effective for demonstrating the abnormality characterized by medial deviation of the lateral nasal walls at the anterior nasal apertures (Fig. 3). The hard palate is also malformed with a V-shaped or triangular morphology, appearing narrowed anteriorly. The demonstration of a single maxillary median incisor should prompt further evaluation of the brain for holoprosencephaly with MRI, which occurs in approximately 25% of cases of SMMCI (Fig. 3), and associated pituitary anomalies are identified in 10% to 50% of cases [9, 13]. The nasal manifestations of holoprosencephaly vary depending on the inciting genetic mutation and can be grouped into four categories: 1) proboscis; 2) premaxillary agenesis with median cleft lip and palate and small or absent nose, 3) pyriform aperture stenosis and single maxillary median incisor and 4) midline facial defects without the typical holoprosencephaly defects in brain cleavage (microform) [14]. The management of pyriform aperture stenosis may consist of temporary nasal stenting [12]. It is important to evaluate for the presence of choanal atresia and midnasal stenosis, since these can also be associated with solitary median maxillary central incisor syndrome [8, 9].

Choanal atresia in CHARGE syndrome

Choanal atresia is a congenital obstruction of the posterior nasal apertures. Choanal atresia results from failure of canalization of the buccopharyngeal and oronasal membranes during embryological development and can be unilateral or bilateral. Unilateral cases are more likely to be sporadic in nature. Chromosomal anomalies have been reported to be present in 6% of infants with choanal atresia and associated malformations are present in nearly 50% of the infants without chromosome anomalies, most commonly in the form of CHARGE syndrome [15]. CHARGE syndrome (coloboma, heart defect, atresia choanae, retarded growth and development, genital hypoplasia, ear anomalies/deafness) is associated with mutations of the CHD7 gene (chromodomain helicase DNA protein family) and has an incidence in the range of 0.1–1.2/10,000 [16]. Neuroimaging in patients with CHARGE syndrome can demonstrate choanal atresia, absence or hypoplasia of the olfactory bulbs and olfactory sulci, and optic disc colobomas as well as highly characteristic inner ear abnormalities, such as absent or hypoplastic semicircular canals, small vestibules, malformed cochleae and small internal auditory canals (Fig. 4) [17, 18]. Additional findings include variable hypoplasia or aplasia of cranial nerves seven and eight and hypoplasia or constriction of the basiocciput. Choanal atresia is typically bilateral when seen in CHARGE syndrome [19]. Several other conditions are also associated with choanal atresia or stenosis, including fetal alcohol syndrome and VATER (vertebral, anorectal, tracheoesophagel, renal/radial

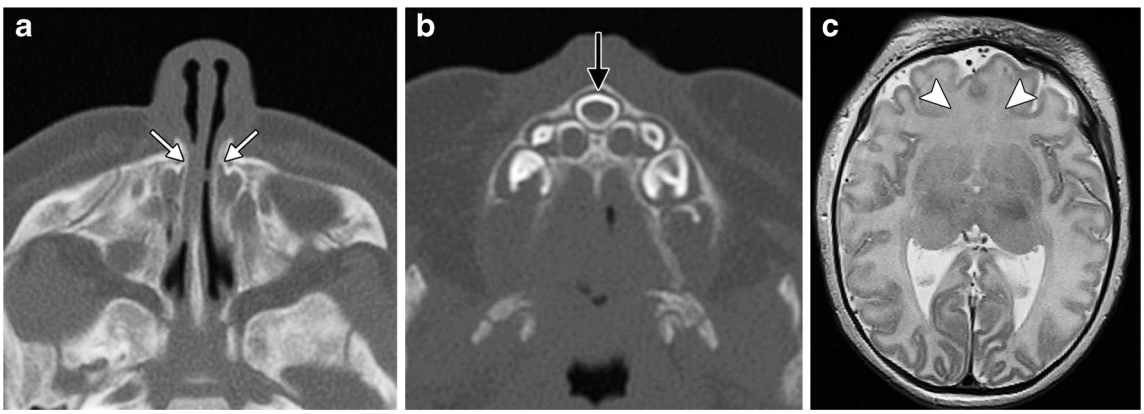

Fig. 3 Solitary median maxillary central incisor syndrome. Day-of-life 1 girl with prenatally diagnosed holoprosencephaly and postnatal nasal obstruction requiring oral intubation. Axial CT image (**a**) shows severe narrowing of the pyriform aperture (*arrows*). Axial CT image (**b**) at a more caudal level shows a central maxillary megaincisor (*black arrow*). Axial T2-weighted MRI of the brain (**c**) shows lack of cleavage of the inferior frontal lobes (*arrowheads*) and reduced separation of the deep grey nuclei across the midline, characteristic of semilobar holoprosencephaly

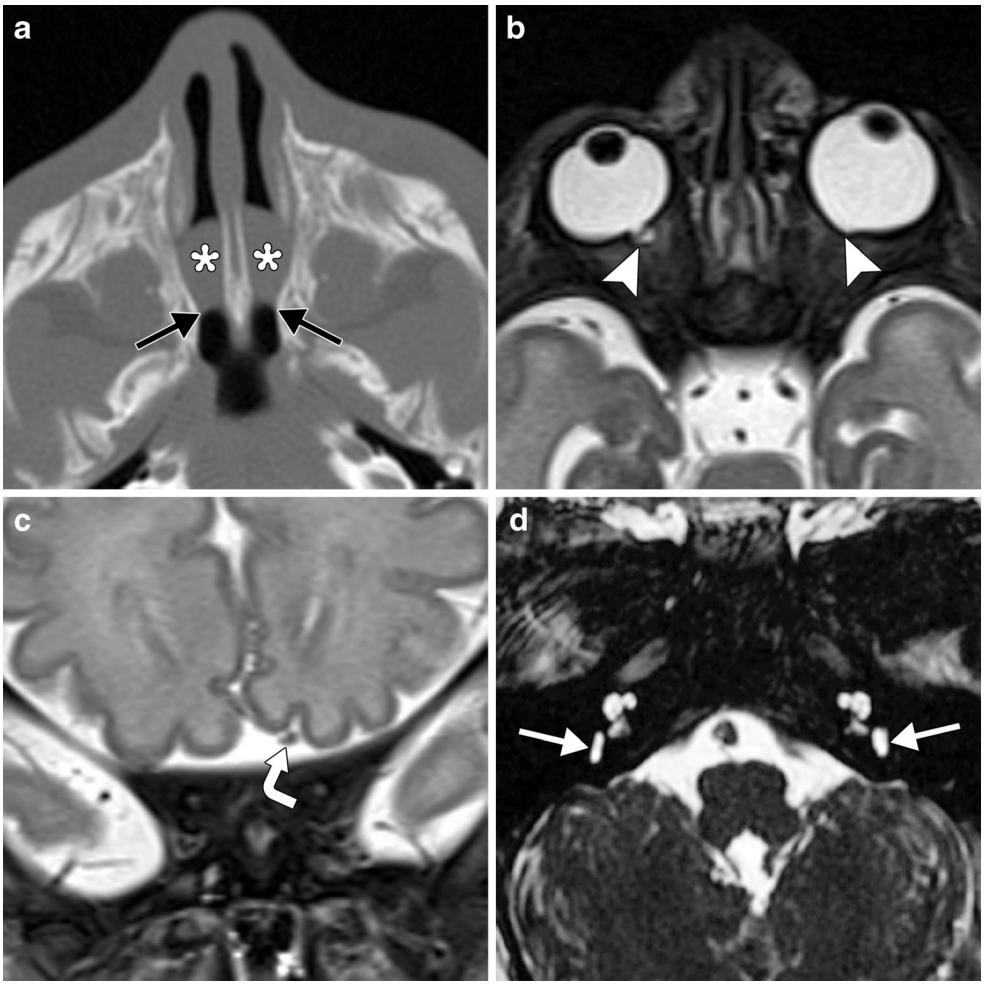

Fig. 4 CHARGE syndrome. Axial CT image in a 6-day-old boy (**a**) shows bilateral bony and membranous choanal atresia with a thickened vomer and medial deviation of the lateral nasal walls at the level of the choanae (*black arrows*). There are secretions layering within the nasal cavities (*). Axial T2-weighted MRI at 4 days of age (same patient) (**b**) shows bilateral colobomas (*arrowheads*). Coronal T2-weighted MRI (**c**) shows that the olfactory apparatus is absent on the right, but intact on the left (*curved arrow*). Axial CISS (constructive interference in steady state) image (**c**) shows bilateral absent semicircular canals and hypoplastic vestibules (*white arrows*). There is also bilateral cochlear nerve aperture and internal auditory canal stenosis

ray) association [20]. Bilateral choanal atresia usually presents as respiratory distress in neonates who are obligate nose breathers. High-resolution thin-section axial CT images parallel to the hard palate confirm the diagnosis of choanal atresia and are useful for treatment planning. The atresia invariably has an osseous component characterized by medial bowing of the posterior lateral nasal wall and thickening of the vomer toward the atretic segment. The atresia is further characterized as entirely osseous or part bony and part membranous in nature. Secretions accumulate anterior to the choanal atresia and should not be mistaken for a mass. Thus, suctioning of the nasal cavity prior to imaging these patients can be useful but should not be performed if the baby is being scanned without sedation and has fallen asleep naturally [21]. Choanal atresia can be successfully managed via transnasal endoscopic repair [22].

Arhinia in Bosma syndrome

The constellation of arhinia (nasal agenesis), microphthalmos, palatal abnormalities, deficient taste and smell, inguinal hernias and hypogonadism with cryptorchidism comprises the rare Bosma arhinia microphthalmia syndrome. The Pax6 gene has been proposed as a candidate gene for this disorder [23, 24]. Maxillofacial CT demonstrates essentially absence of the nasal cavity with nearly confluent bone and complete absence of the external nose resulting in a flattened midface (Fig. 5). Obstruction of the nasolacrimal ducts in association with the absent nasal cavity results in dacryocystoceles. Arhinia with hypotelorism occasionally occurs as a feature of holoprosencephaly. Management of arhinia involves urgent intubation or tracheostomy followed by surgical reconstruction of a nasal airway. The internal nose can be created through maxillary osteotomy and ostectomy and lined with a local skin flap and split-thickness skin grafts, and the external nose can be reconstructed using an expanded frontal flap and bone graft framework [25, 26].

Frontonasal hemangiomas in PHACES association

Segmental neurovascular syndromes ("vascular phakomatoses"), such as PHACES association, have been postulated to result from somatic mutations in the region of

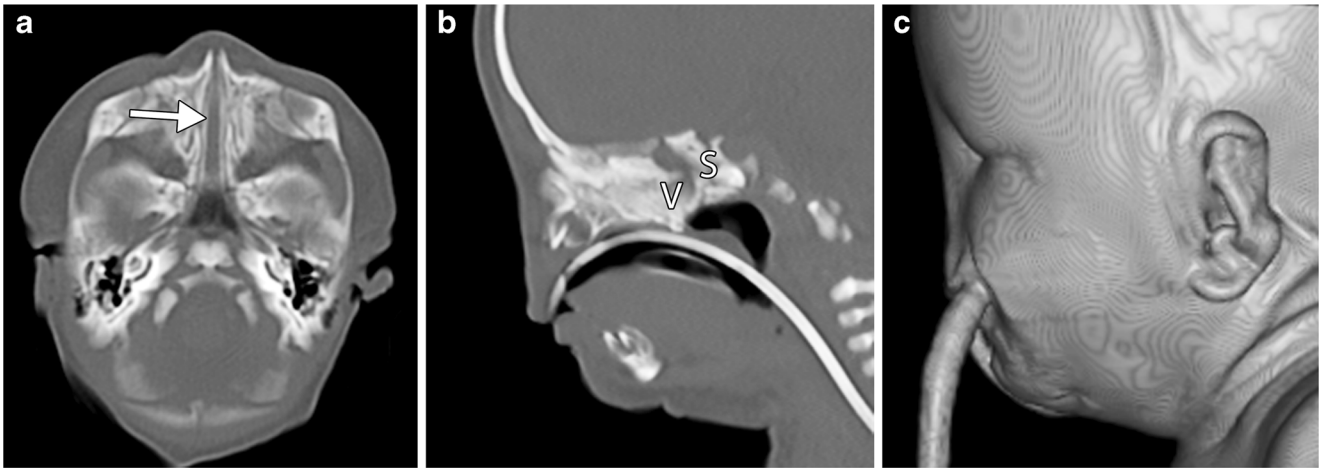

Fig. 5 Bosma syndrome in a 3-day-old boy with congenital absence of the nose. Axial (**a**), sagittal (**b**) and 3-D surface-rendered (**c**) CT images show atresia of the internal nasal cavity (*arrow*), in which the vomer (V) is fused to the sphenoid bone (S). In addition, there is complete absence of the external nose and nostrils. The patient is intubated. The globes were severely microphthalmic (*not shown*)

the neural crest or adjacent cephalic mesoderm that occur prior to migration of these cells [27]. Since migration of these cells normally traverses the brain, cranium and face under the control of HOX genes, the somatic mutations can potentially affect all of these structures within the same metameric (transverse) segment [27]. Neural crest cells also contribute to the development of the heart and trunk, which accounts for associated abnormalities in these areas in certain segmental neurovascular syndromes [27, 28]. The PHACES association consists of posterior fossa malformations (most commonly unilateral cerebellar hypoplasia), hemangiomas, arterial anomalies (coarctation of the aorta and neurovascular malformations), cardiac defects (most commonly ventricular septal defects), eye abnormalities (retinal hypervascularity, glaucoma, morning glory disc anomaly and cataracts) and sternal or ventral defects. Regional, beard-like or midline craniofacial hemangiomas are commonly observed in children with PHACES association and tend to be distributed in the frontotemporal (S1), maxillary (S2), mandibular (S3) and frontonasal regions (S4), in decreasing order of frequency [29]. The overall risk of PHACES association is 31% in patients with facial hemangiomas that are larger than 5 cm [30]. Thus, further imaging with brain MRI and MR angiography is warranted in patients with known or suspected PHACES association to evaluate intracranial malformations (Fig. 6). Associated intracranial malformations include additional hemangiomas that are most commonly located in the internal auditory canals, Dandy-Walker spectrum (uncommon), cerebellar hemisphere

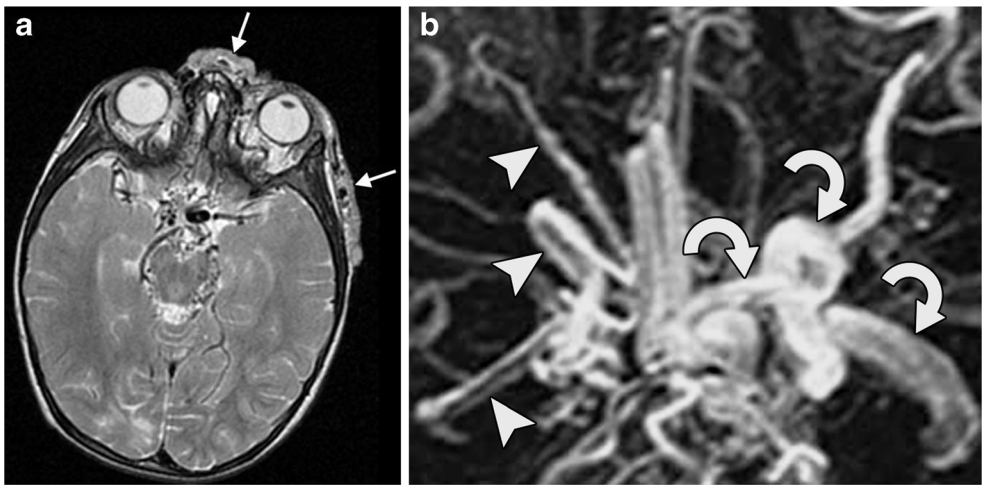

Fig. 6 PHACES association in a 9-week-old girl with plaque-like masses in the face. Axial T2 MRI (**a**) shows plaque-like hemangiomas in the midline frontonasal and left frontotemporal subcutaneous tissues (*arrows*). There are also abnormal flow voids in the circle of Willis. Maximum intensity projection time-of-flight circle of Willis MR angiography (**b**) shows significant steno-occlusive lesions affecting the right internal carotid artery and its branches (*arrowheads*) versus an ectatic, tortuous left internal carotid artery and branches (*curved arrows*). Associated moyamoya collateral vessels are also present on the right side

hypoplasia ipsilateral to the hemangioma, cortical malformation, hypogenesis of the corpus callosum and arachnoid cysts [31, 32]. Neurovascular anomalies related to PHACES may include hypoplasia or agenesis of major cerebral vessels, persistence of embryonic vessels, progressive vascular stenosis or occlusion, and ectasia and tortuosity of the cerebral vasculature [31].

Bifid nose in median cleft face syndrome (frontonasal dysplasia, craniofrontonasal dysplasia, Burian syndrome)

Median cleft face syndrome has a wide range of phenotypic expressions that can be sporadic or associated with a gene deletion on chromosome 21q22.3 or a mutation of the Ephrin-B1 (EFNB1) gene on the X chromosome, depending upon the particular type [33, 34]. In addition, frontonasal dysplasia is associated with increased expression of the sonic hedgehog protein (SHH), in contrast to the decreased expression of SHH that characterizes holoprosencephaly [4]. This translates into frontonasal dysplasia with absent or deficient medial nasal prominence derivatives during embryogenesis. Consequently, bifid nose is frequently associated with other midline facial clefts and hypertelorism. Furthermore, neuroimaging may reveal associated craniosynosotosis, callosal dysgenesis, basal encephaloceles and persistent craniopharyngeal canal (Fig. 7) [34–36]. Craniopharyngeal canals are well-corticated defects in the midline of the sphenoid bone that extend from the sellar floor to the anterosuperior nasopharyngeal roof and can be classified as incidental canals, canals with ectopic adenohypophysis, and canals containing cephaloceles or tumors [37]. Patients often benefit from reconstructive maxillofacial surgery. In particular, the bifid nose deformity can be corrected via rhinoplasty, which may require extensive skin, bony and cartilaginous resection and reconstruction [38, 39].

Lateral nasal clefts in Bartsocas-Papas syndrome (popliteal pterygium syndrome)

Bartsocas-Papas syndrome or sequence is an autosomal recessive condition related to a mutation in the Interferon Regulatory Factor 6 (IRF6) gene or receptor-interacting serine-threonine kinase 4 (RIPK4) gene [40–42]. The genetic defects lead to ectodermal necrosis in the embryo. Consequently, the main findings include webbing of the skin, syndactyly, orofacial clefts including the cleft in the lateral part of the nose (nasoschizis), oral filiform bands, ankyloblepharon and short palpebral fissures, nasal and oral cavity hypoplasia and deformity, and microcephaly [42]. Maxillofacial CT is useful for characterizing the complex bilateral orofacial clefts and midface hypoplasia if reconstructive surgery is contemplated among patients who survive into childhood and beyond (Fig. 8).

Nasofrontal mass in duplication of the pituitary gland-plus syndrome

Duplication of the pituitary gland-plus syndrome comprises a continuum of developmental anomalies of the median line that occur during blastogenesis, of which pituitary gland duplication is a salient manifestation [43]. Since the notochord induces formation of the pituitary plaque, a split notochord of the prechordal plate could also lead to duplication of the hypophysis. The syndrome ranges in severity and may include midline lesions, such as clival encephalocele, third cerebral peduncle, duplicate odontoid process, facial cleft, double tongue, cleft palate, hypertelorism, callosal dysgenesis, hypothalamic enlargement, fenestrated basilar artery, supernumerary teeth and nasofrontal or oral masses,

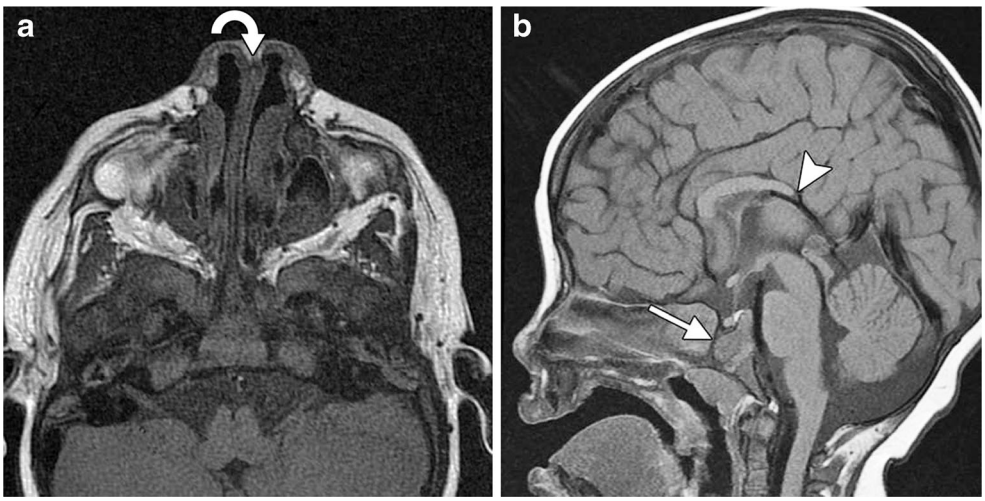

Fig. 7 Median cleft face syndrome with bifid nose in a 3-year-old girl with cosmetic deformity due to nasal malformation and left unilateral craniosynostosis. Axial T1-weighted MRI (**a**) shows a wide gap between the medial portions of the lateral nasal cartilages (*curved arrow*). Sagittal T1-weighted MRI (**b**) shows a persistent craniopharyngeal canal (*arrow*) and corpus callosum hypogenesis (*arrowhead*)

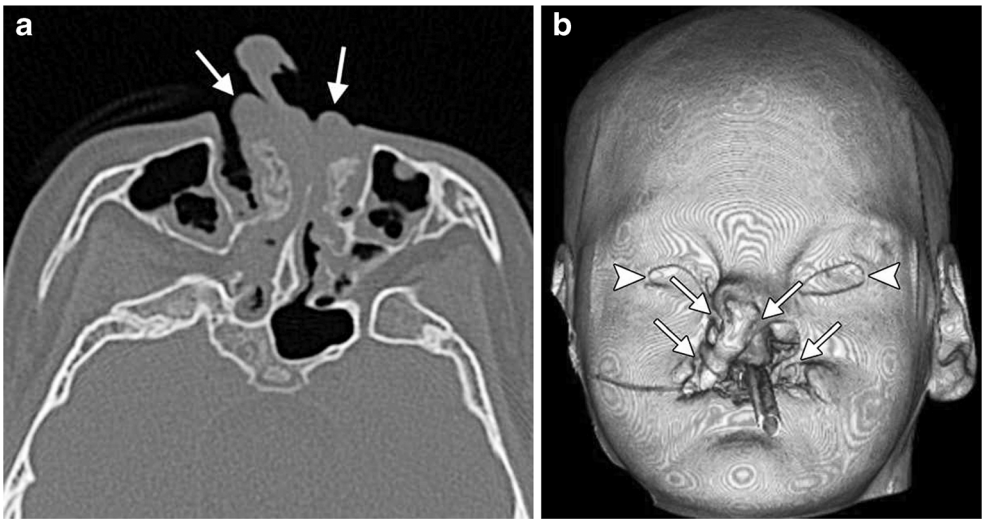

Fig. 8 Bartsocas-Papas syndrome in a 13-year-old girl with facial clefts and syndactyly. Axial (**a**) and 3-D volume-rendered (**b**) CT images show a deformed, hypoplastic nose and nasal cavity, bilateral orofacial clefts through which the inferior turbinates protrude (*arrows*). The 3-D image also shows a small, deformed mouth and short palpebral fissures (*arrowheads*)

including teratomas, hamartomas, epidermoids and dermoids, which should be evaluated via head and neck imaging (Fig. 9) [44–48]. The midline nasofrontal masses can communicate with the anterior cranial fossa via a patent foramen cecum or fonticulus frontalis [49]. Failure of involution at these sites where surface and neural ectoderm approximate each other can lead to anomalous development including nasal dermal sinus, encephalocele and nasal glioma [7]. In very extreme cases, there can be complete duplication of the maxillofacial structures, which is known as diprosopus.

Nasal hypoplasia in craniofacial syndromes

Craniosynostosis and midface hypoplasia are the salient features of several craniofacial syndromes, including Antley-Bixler, Apert and Crouzon syndromes, among others, and result from insufficient formation or migration of mesenchyme to the skull base and face [49–51]. The midfacial hypoplasia in these syndromes is associated with nasal dorsum retrusion, narrowing of the midnasal cavity, shallow orbits with exorbitism, hypertelorism and hypopneumatization of the maxillary sinuses. Skull base anomalies are also ubiquitous features of the craniofacial syndromes and may include external auditory canal stenosis or atresia, basilar invagination, foramen magnum stenosis and jugular foraminal stenosis or atresia with associated prominent basal emissary foramina [52]. High-resolution CT with multiplanar reformatted images and 3-D surface renderings are useful for analysis abnormalities of the calvarium, nasal bones and maxilla in terms of surgical planning (Fig. 10) [53]. MRI is more useful than CT for evaluating intracranial abnormalities, which can include

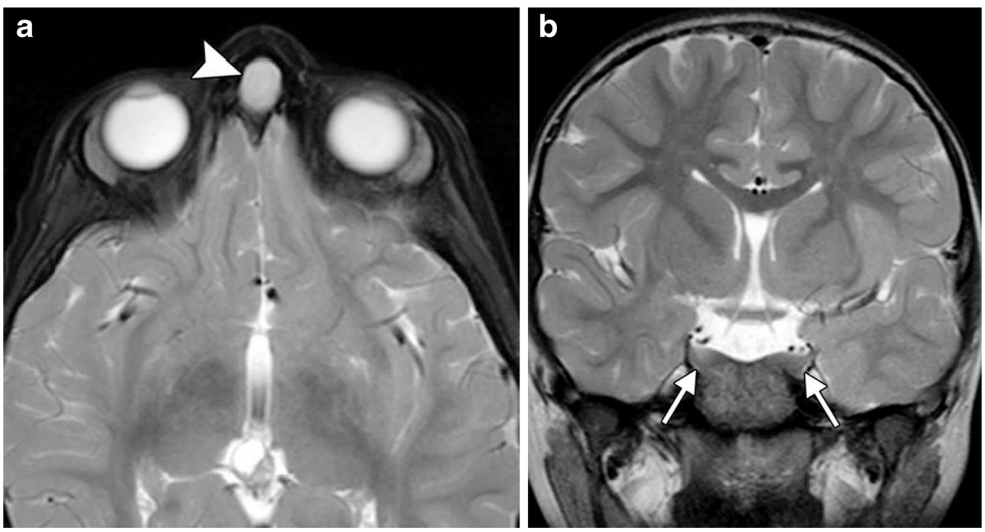

Fig. 9 Duplication of the pituitary gland-plus syndrome in an infant with nasal dermal sinus. T2-weighted MR (**a**) axial image shows a hyperintense, circumscribed, oval lesion within an enlarged foramen cecum (*arrowhead*). **b** Coronal image demonstrates two laterally positioned sellae each containing a pituitary gland and infundibulum (*arrows*). Courtesy of Dr. Christopher Filippi

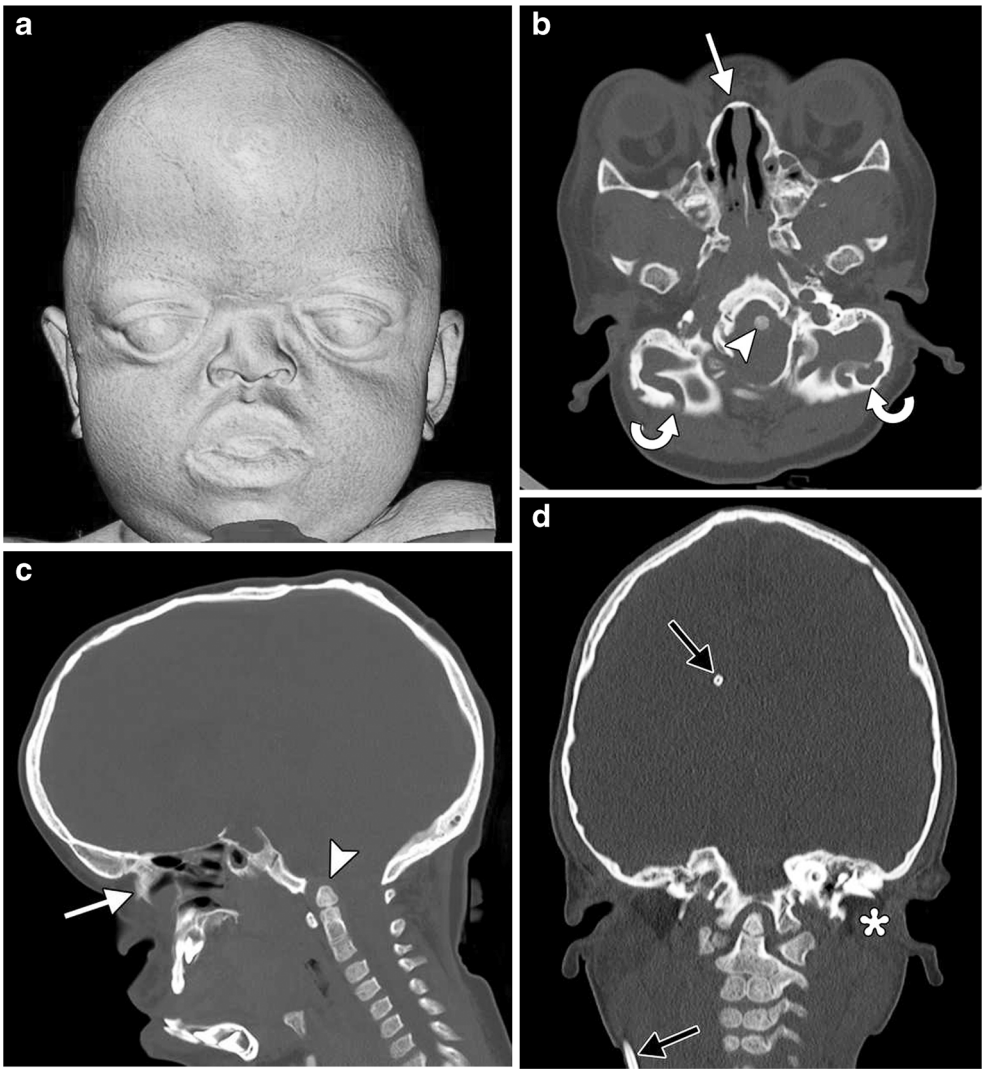

Fig. 10 Craniofacial syndrome in a 2-year-old girl with Crouzon syndrome. Three-dimensional surface-rendering (**a**), axial (**b**), sagittal (**c**) and coronal (**d**) CT images show midface hypoplasia with a retruded nasal bridge (*white arrows*), brachycephaly, and skull bases anomalies, including basilar invagination (*arrowheads*), enlarged occipitomastoid emissary foramina (*curved arrows*) and external auditory canal atresia (*). The child also underwent ventriculoperitoneal shunting (*black arrows*) for hydrocephalus

ventriculomegaly and hydrocephalus, callosal anomalies, hypoplasia/absence of the septum pellucidum, hypoplasia/dysplasia of the hippocampus, distortion or less commonly malformation of the cerebral cortex, and Chiari I malformation [51]. Since staged operations are often performed to successively correct extensive craniofacial malformations, imaging is useful for planning subsequent additional surgical reconstruction and the postoperative changes should be recognized on imaging [54, 55].

Conclusion

Congenital nasal lesions may represent only the tip of the iceberg in patients with syndromic diseases. Radiologic evaluation plays an important role in evaluating associated brain, maxillofacial and cerebrovascular anomalies.

Conflicts of interest None

References

1. Ginat DT, Robson CD (2014) Diagnostic imaging features of congenital nose and nasal cavity lesions. Clin Neuroradiol. doi:10.1007/s00062-014-0323-5
2. Etchevers HC, Couly G, Vincent C et al (1999) Anterior cephalic neural crest is required for forebrain viability. Development 126: 3533–3543
3. Som PM, Naidich TP (2013) Illustrated review of the embryology and development of the facial region, part 1: early face and lateral nasal cavities. AJNR Am J Neuroradiol 34:2233–2240
4. Som PM, Streit A, Naidich TP (2014) Illustrated review of the embryology and development of the facial region, part 3: an overview of the molecular interactions responsible for facial development. AJNR Am J Neuroradiol 35:223–229
5. Hengerer AS, Brickman TM, Jeyakumar A (2008) Choanal atresia: embryologic analysis and evolution of treatment, a 30-year experience. Laryngoscope 118:862–866

6. Nemzek WR, Brodie HA, Hecht ST et al (2000) MR, CT, and plain film imaging of the developing skull base in fetal specimens. AJNR Am J Neuroradiol 21:1699–1706
7. Hedlund G (2006) Congenital frontonasal masses: developmental anatomy, malformations, and MR imaging. Pediatr Radiol 36:647–662, quiz 726-727
8. Hall RK (2006) Solitary median maxillary central incisor (SMMCI) syndrome. Orphanet J Rare Dis 1:12
9. Nanni L, Ming JE, Du Y et al (2001) SHH mutation is associated with solitary median maxillary central incisor: a study of 13 patients and review of the literature. Am J Med Genet 102:1–10
10. Tate JR, Sykes J (2009) Congenital nasal pyriform aperture stenosis. Otolaryngol Clin N Am 42:521–525
11. Belden CJ, Mancuso AA, Schmalfuss IM (1999) CT features of congenital nasal pyriform aperture stenosis: initial experience. Radiology 213:495–501
12. Lee KS, Yang CC, Huang JK et al (2002) Congenital pyriform aperture stenosis: surgery and evaluation with three-dimensional computed tomography. Laryngoscope 112:918–921
13. Van Den Abbeele T, Triglia JM, François M et al (2001) Congenital nasal pyriform aperture stenosis: diagnosis and management of 20 cases. CNPAS has been reported to have an association with a single maxillary central incisor in up to 60% of cases. Ann Otol Rhinol Laryngol 110:70–75
14. Mercier S, Dubourg C, Garcelon N et al (2011) New findings for phenotype-genotype correlations in a large European series of holoprosencephaly cases. J Med Genet 48:752–760
15. Harris J, Robert E, Källén B (1997) Epidemiology of choanal atresia with special reference to the CHARGE association. Pediatrics 99:363–367
16. Blake KD, Prasad C (2006) CHARGE syndrome. Orphanet J Rare Dis 1:34
17. Morimoto AK, Wiggins RH 3rd, Hudgins PA et al (2006) Absent semicircular canals in CHARGE syndrome: radiologic spectrum of findings. AJNR Am J Neuroradiol 27:1663–1671
18. Blustajn J, Kirsch CF, Panigrahy A et al (2008) Olfactory anomalies in CHARGE syndrome: imaging findings of a potential major diagnostic criterion. AJNR Am J Neuroradiol 29:1266–1269
19. Keller JL, Kacker A (2000) Choanal atresia, CHARGE association, and congenital nasal stenosis. Otolaryngol Clin N Am 33:1343–51
20. Lowe LH, Booth TN, Joglar JM et al (2000) Midface anomalies in children. Radiographics 20:907–922, quiz 1106-1107, 1112
21. Teissier N, Kaguelidou F, Couloigner V et al (2008) Predictive factors for success after transnasal endoscopic treatment of choanal atresia. Arch Otolaryngol Head Neck Surg 134:57–61
22. Black CM, Dungan D, Fram E et al (1998) Potential pitfalls in the work-up and diagnosis of choanal atresia. AJNR Am J Neuroradiol 19:326–329
23. Graham JM Jr, Lee J (2006) Bosma arhinia microphthalmia syndrome. Am J Med Genet A 140:189–193
24. Bosma JF, Henkin RI, Christiansen RL et al (1981) Hypoplasia of the nose and eyes, hyposmia, hypogeusia, and hypogonadotrophic hypogonadism in two males. J Craniofac Genet Dev Biol 1:153–184
25. Meyer R (1997) Total external and internal construction in arhinia. Plast Reconstr Surg 99:534–542
26. Brusati R, Donati V, Marelli S et al (2009) Management of a case of arhinia. J Plast Reconstr Aesthet Surg 62:e206–210
27. Krings T, Geibprasert S, Luo CB et al (2007) Segmental neurovascular syndromes in children. Neuroimaging Clin N Am 17:245–258
28. Keyte A, Hutson MR (2012) The neural crest in cardiac congenital anomalies. Differentiation 84:25–40
29. Rudnick EF, Chen EY, Manning SC et al (2009) PHACES syndrome: otolaryngic considerations in recognition and management. Int J Pediatr Otorhinolaryngol 73:281–288
30. Haggstrom AN, Garzon MC, Baselga E et al (2010) Risk for PHACE syndrome in infants with large facial hemangiomas. Pediatrics 126:e418–e426
31. Judd CD, Chapman PR, Koch B et al (2007) Intracranial infantile hemangiomas associated with PHACE syndrome. AJNR Am J Neuroradiol 28:25–29
32. Oza VS, Wang E, Berenstein A et al (2008) PHACES association: a neuroradiologic review of 17 patients. AJNR Am J Neuroradiol 29:807–813
33. Bhattacharya JJ, Luo CB, Suh DC et al (2001) Wyburn-Mason or Bonnet-Dechaume-Blanc as Cerebrofacial Arteriovenous Metameric Syndromes (CAMS). A new concept and a new classification. Interv Neuroradiol 7:5–17
34. Guion-Almeida ML, Richieri-Costa A, Jehee FS et al (2004) Frontonasal dysplasia, callosal agenesis, basal encephalocele, and eye anomalies syndrome with a partial 21q22.3 deletion. Proc Natl Acad Sci U S A 101:8652–8657
35. Núñez-Villaveirán T, Frohner BB, Urcelay PR et al (2013) Bifid nose - a mild degree of frontonasal dysplasia. A case report. Int J Pediatr Otorhinolaryngol 77:1374–1377
36. Sharma S, Sharma V, Bothra M (2013) Frontonasal dysplasia (Median cleft face syndrome). J Neurosci Rural Pract 3:65–67
37. Abele TA, Salzman KL, Harnsberger HR et al (2014) Craniopharyngeal canal and its spectrum of pathology. AJNR Am J Neuroradiol 35:772–777
38. Twigg SR, Kan R, Babbs C et al (2004) Mutations of ephrin-B1 (EFNB1), a marker of tissue boundary formation, cause craniofrontonasal syndrome. Proc Natl Acad Sci U S A 101:8652–8657
39. Miller PJ, Grinberg D, Wang TD (1999) Midline cleft. Treatment of the bifid nose. Arch Facial Plast Surg 1:200–203
40. Veenstra-Knol HE, Kleibeuker A, Timmer A et al (2003) Unreported manifestations in two Dutch families with Bartsocas-Papas syndrome. Am J Med Genet A 123A:243–248
41. Gripp KW, Ennis S, Napoli J (2013) Exome analysis in clinical practice: expanding the phenotype of Bartsocas-Papas syndrome. Am J Med Genet A 161A:1058–1063
42. Mitchell K, O'Sullivan J, Missero C et al (2012) Exome sequence identifies RIPK4 as the Bartsocas-Papas syndrome locus. Am J Hum Genet 90:69–75
43. Manjila S, Miller EA, Vadera S et al (2012) Duplication of the pituitary gland associated with multiple blastogenesis defects: duplication of the pituitary gland (DPG)-plus syndrome. Case report and review of literature. Surg Neurol Int 3:23
44. Chariker M, Ford R, Morrison C et al (2011) Pituitary duplication with nasopharyngeal teratoma and cleft palate. J Craniofac Surg 22:755–758
45. Huisman TA, Fischer U, Boltshauser E et al (2005) Pituitary duplication and nasopharyngeal teratoma in a newborn: CT, MRI, US and correlative histopathological findings. Neuroradiology 47:558–561
46. Ginat DT, Holbrook EH, Faquin W et al (2013) Nasal hamartoma associated with duplicated pituitary. J Comput Assist Tomogr 37:369–370
47. Uchino A, Sawada A, Takase Y et al (2002) Extreme fenestration of the basilar artery associated with cleft palate, nasopharyngeal mature teratoma, and hypophyseal duplication. Eur Radiol 12:2087–2090
48. Mutlu H, Paker B, Gunes N et al (2004) Pituitary duplication associated with oral dermoid and corpus callosum hypogenesis. Neuroradiology 46:1036–1038

49. Lowe LH, Booth TN, Joglar JM et al (2000) Midface anomalies in children. Radiographics 20:907–922, quiz 1106-1107, 1112
50. McGlaughlin KL, Witherow H, Dunaway DJ et al (2010) Spectrum of Antley-Bixler syndrome. J Craniofac Surg 21: 1560–1564
51. Tokumaru AM, Barkovich AJ, Ciricillo SF et al (1996) Skull base and calvaria deformities: association with intracranial changes in craniofacial syndromes. AJNR Am J Neuroradiol 17:619–630
52. Robson CD, Mulliken JB, Robertson RL et al (2000) Prominent basal emissary foramina in syndromic craniosynostosis: correlation with phenotypic and molecular diagnoses. AJNR Am J Neuroradiol 21: 1707–1717
53. Sannomiya EK, Reis SA, Asaumi J et al (2006) Clinical and radiographic presentation and preparation of the prototyping model for pre-surgical planning in Apert's syndrome. Dento Maxillofac Radiol 35:119–124
54. Marchac D, Renier D, Broumand S (1994) Timing of treatment for craniosynostosis and faciocraniosynostosis: a 20-year experience. Br J Plast Surg 47:211–222
55. Schatz CJ, Ginat DT (2013) Imaging features of rhinoplasty. AJNR Am J Neuroradiol 35:216–222